Water Research X 24 (2024) 100233

Contents lists available at ScienceDirect

Water Research X

journal homepage: www.sciencedirect.com/journal/water-research-x

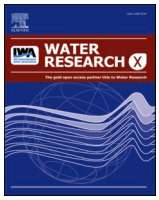

Effects of functional groups of polyfluoroalkyl substances on their removal by nanofiltration

Takahiro Fujioka [a,*], Haruka Takeuchi [b], Hironobu Tahara [a], Hiroto Murakami [a], Sandrine Boivin [a]

[a] Graduate School of Integrated Science and Technology, Nagasaki University, 1-14 Bunkyo-machi, Nagasaki 852-8521, Japan
[b] Research Center for Environmental Quality Management, Kyoto University, 1-2 Yumihama, Otsu 520-0811, Japan

ARTICLE INFO

Keywords:
Nanofiltration membrane
Contaminants of emerging concern
Micropollutants
Polypiperazine-amide
Perfluoroalkyl sulfonates
PFAS

ABSTRACT

Determining the reliability of nanofiltration (NF) membranes for the removal of contaminants of emerging concern, including polyfluoroalkyl substances (PFASs), pharmaceuticals, and personal care products (PPCPs), is important for ensuring drinking water safety. This study aimed to clarify the factors that influence the removal of nine major PFASs during submerged NF treatment via extrapolation based on the factors that influence PPCP removal. The rejection of nine PFASs in ultra-filtered dam water by a polypiperazine-amide (NF270) membrane increased from 71 % to 94 % at a low permeate flux of 5 L/m^2 h as the PFAS molecular dimensions increased. PFASs with a carboxylic acid (-CO_2H) were rejected to a greater extent than PFASs with a sulfo group (-SO_3H). Further, negatively charged PFASs or PPCPs were rejected to a greater extent than uncharged and positively charged PPCPs. Our findings suggest that the rejection of PFASs can vary because of the (i) clearance distance between the PFASs' molecular dimensions and NF membrane pore diameter and (ii) intensity of electrostatic repulsion between the PFASs' functional groups and NF membrane surface. Our study indicates that submerged NF can achieve high PFAS rejection; however, variations in rejection among PFASs can become more prominent owing to a low permeate flux.

1. Introduction

Trace organic chemicals (TOrCs), particularly perfluoroalkyl substances (PFASs), pharmaceuticals, and personal care products (PPCPs), are challenging contaminants that have caused increasing concern regarding their threat to the safety of drinking water (Bieber et al., 2018). Among advanced drinking water treatment processes, nanofiltration (NF) membranes with a typical molecular weight cut-off of 150–2000 g/mol (Boussu et al., 2006; Mohammad et al., 2015) represent a powerful separation technology that can remove most chemicals. Because the molecular weight (MW) of PPCPs (200–1000 g/mol) is equivalent to the pore diameter, TOrC rejection by NF membranes can vary considerably depending on the interaction between the membrane surface and TOrCs. The primary rejection mechanisms of TOrCs, including PPCPs, by NF membranes (i.e., size exclusion, electrostatic interaction, and adsorption) have been established in many previous studies (Bellona and Drewes, 2005; Lee et al., 2022; Nghiem et al., 2006; Verliefde et al., 2008a; Wang et al., 2024); thus, whether a chemical will be rejected can be estimated based on its physicochemical properties. However, PFAS rejection trends may differ from PPCP rejection trends due to the differences in chemical structure between PFASs and PPCPs (aliphatic and aromatic compounds, respectively).

High (>95 %) PFAS rejection by NF membranes has been reported previously (Zhi et al., 2022), except for some PFASs such as perfluorooctane sulfonamide (PFOSA) (72 % by NF270) (Steinle-Darling and Reinhard, 2008) or perfluorooctanoate (PFBA) (85 % by NF90) (Li et al., 2021). Furthermore, most previous studies have focused on removing two major PFASs in water environments, namely, perfluorooctanoic acid (PFOA) and perfluorooctanesulfonic acid (PFOS) (Abbasian Chaleshtari and Foudazi, 2022; Liu et al., 2022; Mastropietro et al., 2021; Zeidabadi et al., 2023). Interestingly, many studies (Li et al., 2021; Liu et al., 2021; Pramanik et al., 2017; Safulko et al., 2023; Toure and Anwar Sadmani, 2019) have found that the rejection of low MW (413 g/mol, carboxylate ion) PFOA was higher than that of high MW (499 g/mol, sulfonate ion) PFOS. However, owing to an insufficient understanding of the mechanisms underlying PFAS rejection by NF

* Corresponding author.
E-mail address: tfujioka@nagasaki-u.ac.jp (T. Fujioka).

https://doi.org/10.1016/j.wroa.2024.100233
Received 2 May 2024; Received in revised form 22 June 2024; Accepted 2 July 2024
Available online 3 July 2024

membranes, the causes of the differences in rejection between PFOA and PFOS have not been clarified.

The rejection of TOrCs, including PFASs and PPCPs, by NF membranes can vary considerably depending on the specific NF operating conditions. For example, operating the NF process at a low permeate flux can reduce energy consumption, although a considerable reduction in the rejection of low MW TOrCs also occurs (Fujioka et al., 2012; Tang et al., 2007). Moreover, a low permeate flux (e.g., 5 L/m^2/h) must be applied for submerged NF membrane treatments owing to the maximum (≈ 1 bar) transmembrane pressure (TMP) (Fujioka et al., 2021; Zhou et al., 2023). Our previous study (Boivin and Fujioka, 2024) demonstrated that submerged flat-sheet NF membrane treatment could enable the omission of the pre-treatment (e.g., microfiltration) process for surface water treatment. In addition, the submerged treatment induced less membrane fouling due to its low permeate flux. The other advantages over pressurized NF systems include requirements for low-pressure pumps and plastic pipes and the fact that pressure vessels are not required to install NF membrane elements. However, assessments of PFAS rejection by NF membranes in the literature have been predominantly performed at high pressure and cross-flow orientations designed for spiral-wound NF membrane elements. Therefore, the fate of PFASs during submerged NF membrane treatment remains unclear.

This study aimed to clarify the factors affecting variable PFAS rejection during submerged nanofiltration of dam water. In particular, we evaluated the rejection of nine PFASs, including five perfluoroalkyl carboxylates (PFCAs) and three perfluoroalkyl sulfonates (PFSAs), using

Table 1
Physicochemical characteristics of the evaluated PFASs and PPCPs at pH 7.5. The properties were obtained using MarvinSketch software (ChemAxon; Budapest, Hungary).

			Formula at pH7.5	MW [Da]	MPA [Å^2] at pH 7.5*	Ionization [%]	Log*D*
PFASs (Negatively Charged)	Carboxylates (PFCAs)	PFHxA	$C_6F_{11}O_2^-$	313	30.0	100	0.18
		PFHpA	$C_7F_{13}O_2^-$	363	32.1	100	0.88
		PFOA	$C_8F_{15}O_2^-$	413	33.8	100	1.58
		PFNA	$C_9F_{17}O_2^-$	463	35.7	100	2.28
		PFDA	$C_{10}F_{19}O_2^-$	513	35.6	100	2.99
	Sulfonates (PFSAs)	PFBS	$C_4F_9O_3S^-$	299	31.2	100	0.25
		PFHxS	$C_6F_{13}O_3S^-$	399	33.6	100	1.65
		PFOS	$C_8F_{17}O_3S^-$	499	34.2	100	3.05
	Ether acid	Gen-X	$C_6HF_{11}O_3^-$	330	32.9	100	0.47
PPCPs	Uncharged & hydrophilic	Acetaminophen	$C_8H_9NO_2$	151	19.9	0	0.90
		Ethenzamide	$C_9H_{11}NO_2$	165	30.3	0	1.02
		Antipyrine	$C_{11}H_{12}N_2O$	188	32.2	0	1.22
		DEET	$C_{12}H_{17}NO$	191	36.9	0	2.50
		Caffeine	$C_8H_{10}N_4O_2$	194	28.3	0	-0.55
		Crotamiton	$C_{13}H_{17}NO$	203	37.8	0	3.09
		Primidone	$C_{12}H_{14}N_2O_2$	218	39.0	0	1.12
		Isopropylantipyrine	$C_{14}H_{18}N_2O$	230	38.1	0	2.35
		Carbamazepine	$C_{15}H_{12}N_2O$	236	39.9	0	2.77
		Cyclophosphamide	$C_7H_{15}Cl_2N_2O_2P$	261	44.6	0	0.10
		Griseofulvin	$C_{17}H_{17}ClO_6$	353	51.9	0	2.17
		Thiamphenicol	$C_{12}H_{15}Cl_2NO_5S$	356	50.6	0	-0.22
	Uncharged & hydrophobic	Triclosan	$C_{12}H_7Cl_3O_2$	290	39.9	40 (-)	4.76
		Triclocarban	$C_{13}H_9Cl_3N_2O$	316	47.9	0	4.93
	Positively charged	Salbutamol	$C_{13}H_{22}NO_3^+$	239	38.2	99	-1.23
		Propranolol	$C_{16}H_{22}NO_2^+$	259	39.0	98	0.82
		Atenolol	$C_{14}H_{23}N_2O_3^+$	266	31.5	98	-1.33
		Disopyramide	$C_{21}H_{30}N_3O^+$	340	64.5	100	0.65
		Sulpiride	$C_{15}H_{24}N_3O_4S^+$	341	51.9	97	-1.17
		Lincomycin	$C_{18}H_{35}N_2O_6S^+$	407	56.6	75	-0.91
		Diltiazem	$C_{22}H_{27}N_2O_4S^+$	415	63.9	83	1.97
		Tiamulin	$C_{28}H_{48}NO_4S^+$	494	81.5	99	2.50
		Clarithromycin	$C_{38}H_{70}NO_{13}^+$	748	107.2	97	1.73
		Azithromycin	$C_{38}H_{74}N_2O_{12}^{2+}$	749	112.4	97	-2.44
		Roxithromycin	$C_{41}H_{77}N_2O_{15}^+$	837	120.1	97	1.41
		Tylosin	$C_{46}H_{78}NO_{17}^+$	916	91.0	89	1.34
	Zwitterion	Norfloxacin	$C_{16}H_{18}FN_3O_3$	319	41.9	91	-0.87
		Ciprofloxacin	$C_{17}H_{18}FN_3O_3$	331	42.8	91	-0.76
		Enrofloxacin	$C_{19}H_{22}FN_3O_3$	359	43.7	91	-0.15
		Levofloxacin	$C_{18}H_{20}FN_3O_4$	361	43.1	85	-0.83
		Tetracycline	$C_{22}H_{25}N_2O_8$	444	56.4	98	-3.99
		Chlortetracycline	$C_{22}H_{23}ClN_2O_8$	479	58.7	96	-3.60
	Negatively charged (Carboxylates)	Naproxen	$C_{14}H_{13}O_3^-$	230	33.6	100	-0.08
		Nalidixic acid	$C_{12}H_{11}N_2O_3^-$	232	33.7	90	0.21
		Mefenamic acid	$C_{15}H_{14}NO_2^-$	241	39.5	100	2.23
		Fenoprofen	$C_{15}H_{13}O_3^-$	242	38.2	100	0.47
		Ketoprofen	$C_{16}H_{13}O_3^-$	254	39.5	100	0.40
		Diclofenac	$C_{14}H_{10}Cl_2NO_2^-$	296	43.6	100	1.05
		Indometacin	$C_{19}H_{15}ClNO_4^-$	358	47.7	100	0.55
		Bezafibrate	$C_{19}H_{19}ClNO_4^-$	362	33.3	100	0.69
	Negatively charged (sulfonamides)	Sulfamethoxazole	$C_{10}H_{10}N_3O_3S^-$	253	42.2	98	-0.08
		Sulfathiazole	$C_9H_8N_3O_2S_2^-$	255	40.1	98	0.08
		Sulfamerazine	$C_{11}H_{12}N_4O_2S^-$	264	46.3	76	0.03
		Sulfadimidine	$C_{11}H_{11}N_4O_2S^-$	278	34.3	76	0.16
		Sulfamonomethoxine	$C_{11}H_{11}N_4O_3S^-$	280	42.5	69	0.33
		Sulfadimethoxine	$C_{12}H_{14}N_4O_4S^-$	310	37.2	80	0.73

* MPAs of the compounds were calculated using their ionized or uncharged forms with projection optimization.

a polypiperazine-amide (NF270) membrane. The selected PFASs included PFOA, PFOS, perfluorohexanesulfonic acid (PFHxS), perfluorononanoic acid (PFNA), and hexafluoropropylene oxide dimer acid (HFPO-DA, or GenX), all of which have been regulated in drinking water by the United States Environmental Protection Agency (PFAS Drinking Water Rule). The PFAS rejection mechanisms were further explored by extrapolating the rejection mechanisms of 46 PPCPs based on their physicochemical properties. This study aims to establish criteria for estimating the level of PFAS rejection based on PFAS properties.

2. Results and discussion

2.1. Size exclusion and electrostatic interactions

The rejection of the selected PFASs (Table 1) by the submerged NF membrane module ranged from 71 % to 94 % (Fig. 1**a**). Notably, two distinct linear increasing trends were observed between PFCAs and PFSAs. High rejection (e.g., >90 %) was expected for all PFASs because of the electrostatic repulsion between the negatively charged PFASs **(Supplementary Materials, Figure S1)** and NF membrane surface (zeta potential of approximately -20 mV at pH 8) (Tu et al., 2011). The relatively low rejection of low-MW PFASs can be attributed to the low operating permeate flux (5 L/m^{2}h) in the submerged filtration orientation, in which a limited transmembrane pressure (TMP) of approximately 100 kPa was available. The low PFAS rejection at the low permeate flux was presumably caused by the low permeate volume per unit time against a near-constant solute flux for any permeate volume (Ma et al., 2024; Wijmans and Baker, 1995). In fact, the rejection of PFOAs, PFHxSs, and PFOSs at a high permeate flux of 40 L/m^2/h (88 %–94 %) was higher than that observed at the low permeate flux of 5 L/m^2/h (79 %–90 %) (Fig. 2).

A similar increasing rejection trend with increasing MW was observed for PPCPs (Fig. 1**b**). Each PPCP rejection is shown in the **Supplementary Materials, Figure S2**. Generally, the rejection of positively charged and low-MW PPCPs (MW <300 g/mol) was lower than that of uncharged and negatively charged PPCPs. Positively charged PPCPs can be more concentrated on the membrane surface than in the bulk solution because of the electrostatic attraction force from the

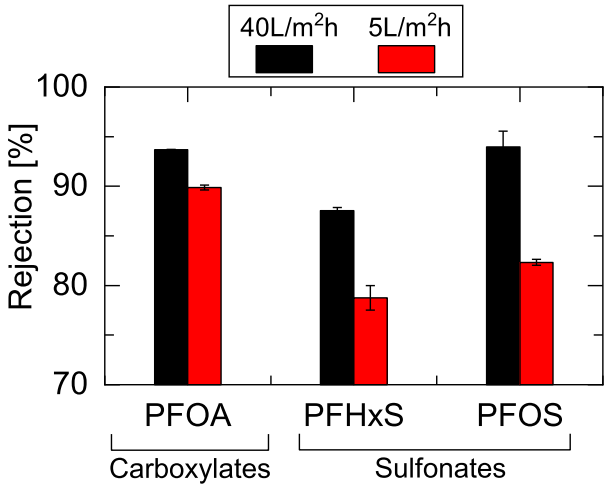

Fig. 2. Rejection of three PFASs by the NF270 membrane at a permeate flux of 40 and 5 L/m^2/h.

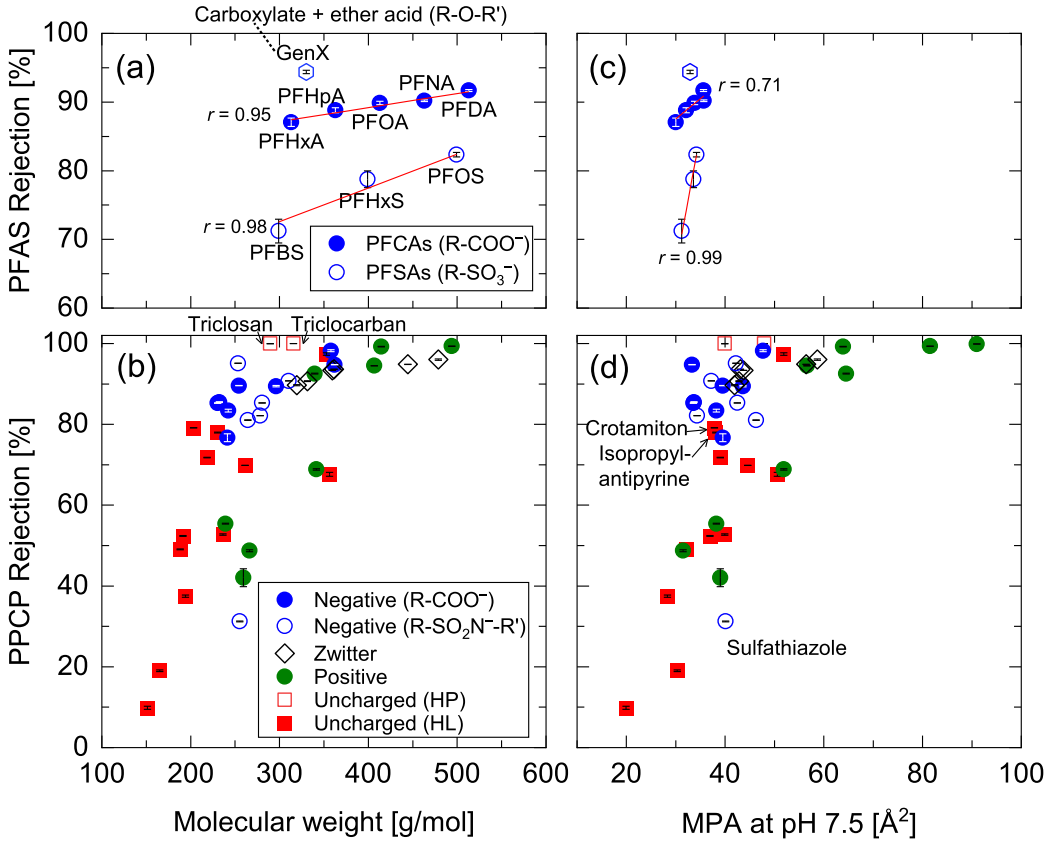

Fig. 1. Rejection of PFASs and PPCPs by the NF270 membrane as a function of (a, b) molecular weight and (c, d) minimum projection area (MPA) at pH 7.5: Carboxylate (R-COO$^-$), sulfonate ion (R-SO$_3^-$), sulfonamide ion (R-SO$_2$N$^-$-R'), hydrophobic (HP), and hydrophilic (HL). Each symbol shows the average and error ranges of duplicated tests after 1 day of NF treatment using ultra-filtered dam water at a permeate flux of 5.0 L/m^{2}h, feed temperature of 22 °C, and TMP of 37 kPa. *r* = Pearson correlation coefficient.

negatively charged NF membrane surface (Verliefde et al., 2008a), which can result in high permeation and low rejection. A distinctly high rejection (99.9 %) was observed for the uncharged and hydrophobic (log*D* = >4.0) PPCPs (triclosan and triclocarban) **(**Fig. 1**b)**. Because their MWs are relatively large (approximately 300 g/mol), they are predominantly rejected and adsorbed on the membrane pores through hydrophobic interactions (Bellona et al., 2004; Verliefde et al., 2008b), thus leading to low concentrations in the permeate (i.e., high rejection). However, the rejection of these hydrophobic chemicals can decrease over time when their adsorption sites on the membrane are occupied (Kimura et al., 2003). Although the typical cut-off value of Log*D* for hydrophobic compounds is 2.0 (Bellona et al., 2004), a high Log*D* cut-off value of 4.0 was used in this study after identifying the remarkable differences that occurred above 2.0 (**Supplementary Materials, Figure S3**). The high cut-off value can be attributed to the lower or almost absent shear force (cross-flow velocity) on the NF membrane surface and low permeate flux, which can reduce adsorption onto the membrane. Compared with uncharged and hydrophilic PPCPs, the rejection of negatively charged PPCPs was generally higher than that of uncharged and positively charged PPCPs. No differences in rejection were observed among PPCPs with different functional groups, such as carboxylic acid and sulfonamide groups.

To confirm the effects of the major separation mechanisms (i.e., size exclusion, electrostatic interaction, and adsorption) on the rejection of PFASs and PPCPs, the rejection data were further analyzed using another dimensional property, the minimum projection area (MPA), which is the area of the compound projection with the minimum plane of its circular disk **(Supplementary Materials, Figure S4)**. The two-dimensional MPA of each compound can be directly associated with the clearance between the compound and membrane pores (Fujioka et al., 2020); thus, compounds smaller than the pore-opening area are more likely to permeate. Our previous study (Fujioka et al., 2019) showed that the MPA could explain the distinct rejection of two similarly structured compounds by a reverse osmosis (RO) membrane (30 % and 88 %) for *N*-nitrosodimethylamine ($C_2H_6N_2O$, MW = 74 g/mol, MPA = 19.4 Å^2) and isobutyraldehyde (C_4H_8O, MW = 72 g/mol, MPA = 22.9 Å^2). In this study, PFSA rejection increased sharply over a short range from 31 to 34 Å^2 MPA, while PFCA rejection remained high regardless of the MPA **(**Fig. 1**c)**. However, the correlation between the MPA of PFCA and NF rejection (Pearson correlation coefficient $r = 0.71$) was lower than that with MWCO ($r = 0.95$), possibly because of the short range of the MPA (MPA = 30.0–35.7 Å^2) compared with that of MWCO (313–513 Da) and similar MPA between PFNA and PFDA (35.7 and 35.6 Å^2, respectively). The rejection of GenX (branched PFAS with a carboxylate ion, MPA = 32.9 Å^2) was higher than any of the PFCAs (MPA = 30.0–35.7 Å^2). Although this result may have been impacted by other structural factors, such as the presence of ether acid **(Supplementary Materials, Figure S1)**, such dynamics were beyond the scope of this study. In the same MPA range, the rejection of negatively charged PPCPs was higher than that of uncharged and positively charged PPCPs **(**Fig. 1**d)**. The rejection of two uncharged and hydrophilic PPCPs (crotamiton and isopropylantipyrine) showed relatively high rejection (78–79 %), likely due to their relatively high hydrophobicity (Log*D* = 3.09 and 2.35, respectively). Notably, the rejection of sulfathiazole, a negatively charged PPCP, was very low (31 %) compared with that of similarly sized PPCPs. Although its uniqueness as a thiazole with a sulfur atom (C_3H_3NS) in its chemical structure might have caused this low rejection, exploring low-rejection PPCPs was beyond the scope of this study. Our findings suggest that negatively charged PFCAs and PPCPs can be highly rejected, likely because of carboxylate ions.

2.2. Role of functional groups

The rejection of negatively charged PFASs and PPCPs by the NF270 membrane was further analyzed to identify the causes of the variability of rejection within each group of compounds. The rejection of PPCPs with a carboxyl acid or a sulfoamide group (R-SO_2N-R') was more variable than that recorded for PFASs **(**Fig. 3**)**. This was attributed to their complex chemical structures and physicochemical properties. For example, mefenamic acid rejection was relatively low (77 %) compared with that of similarly sized PPCPs, likely owing to its relatively high hydrophobicity (Log*D* = 2.2) compared to that of other PPCPs (Log*D* = -0.1–1.1). Further, sulfamerazine rejection was also low (81 %) despite its high molecular dimension (MPA = 46 Å^2), likely because of its relatively low (76 %) dissociation level **(**Table 1**)**. Similar to the findings for negatively charged PPCPs, the rejection of PFASs was higher than that of uncharged and positively charged PPCPs in the MPA range of 30–37 Å^2 **(**Fig. 3**)**. Despite the significant differences in chemical structure between PFASs (aliphatic compounds) and PPCPs (aromatic compounds), negatively charged PFASs and PPCPs did not show a clear difference in rejection in the MPA range of 34–37 Å^2. This implies that the rejection of negatively changed PPCPs and PFASs may show comparatively high levels regardless of their chemical structure. However, PFAS rejection exhibited a clear trend with PFCA rejection.

Specifically, PFCAs (pKa = 0.3–0.4) and PFSAs (pKa = -3.3) are fully dissociated in solution at pH 7.5 and can act as strong acids. Owing to a simple single-chain structure, their MPAs (30–36.6 g/mol) do not vary considerably despite the significant variation in MW (299–513 g/mol). However, MPA values were within the critical range for determining the rejection of uncharged PPCPs **(**Fig. 3**)**. Therefore, in addition to the size exclusion mechanism, electrostatic repulsion is essential for determining whether different PFASs will be rejected. Among similarly sized and negatively charged PFASs and PPCPs (PFOA, PFOS, and nalidxic acid), PFOS had three hydrogen acceptors with a partial negative charge of -0.66 electron units in the gas phase and -0.69 electron units in water medium on each oxygen atom **(Supplementary Materials, Figure S1)**. In contrast, PFOA had two hydrogen acceptors with a partial negative charge holding -0.76 electron units on each oxygen atom in the gas phase and -0.83 electron units in the water medium. The higher partial negative charge of PFOA may represent the primary cause of its higher rejection **(**Fig. 4**)**. This presumption may be supported by the equivalent rejection of nalidixic acid, which presents a high partial negative charge of -0.83 electron units on each oxygen atom in the gas phase and -0.92 electron units in the water medium **(Supplementary Materials, Figure S5)**. The results suggest that PPCPs and PFASs with fully dissociated carboxylate ions can be highly rejected because of high electrostatic repulsion from the carboxylate ions of the NF membranes.

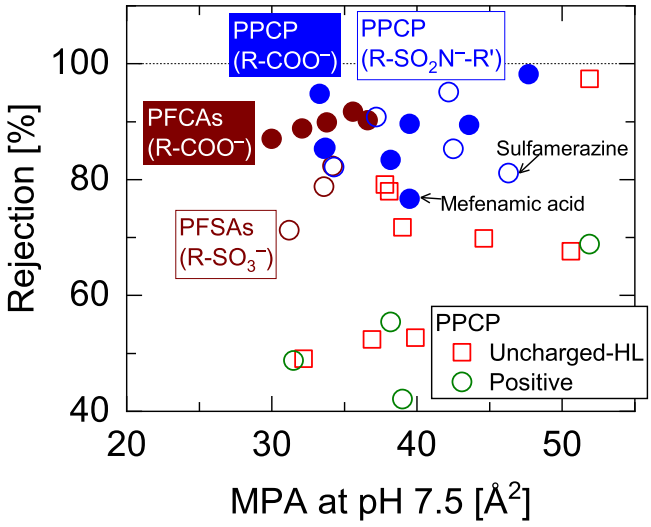

Fig. 3. Rejection of PFASs with a carboxylate (R-COO^-) or a sulfonate ion (R-SO_3^-) and PPCPs with a carboxylate ion or sulfonamide (R-SO_2N-R') group by the NF270 membrane as a function of minimum projection area (MPA) in a solution at pH 7.5.

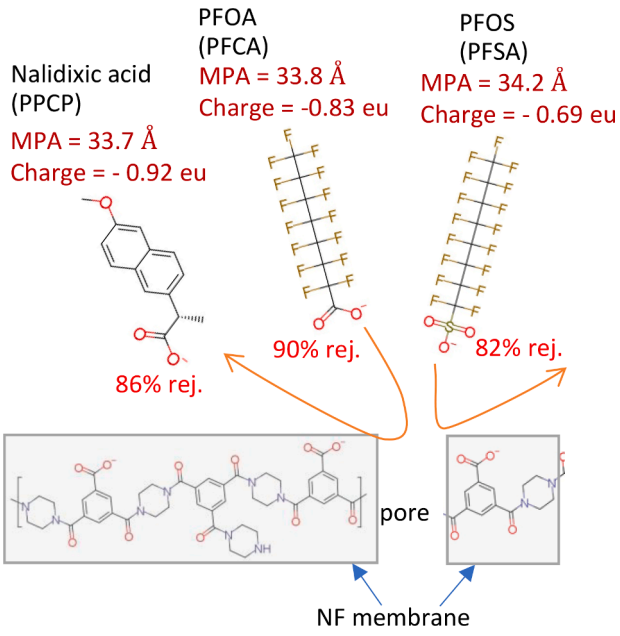

Fig. 4. Conceptual image of differences in rejection among similarly sized and negatively charged PFASs (PFOA and PFOS) and PPCPs (nalidixic acid) due to the differences in their partial negative charge.

2.3. Implications

Previous studies have predominantly evaluated PFAS rejection using high-pressure (i.e., high-permeate flux) NF treatment, which provides high PFAS rejection. In contrast, the low permeate flux adopted in this study enabled the evaluation of variations in PFAS rejection. It should be noted that using only one relatively loose NF membrane (NF270) represents a limitation of this study because the rejection of TOrCs, including PFASs, can vary depending on the selection of NF membranes. Further, because PFAS rejection by submerged NF treatment is lower than that by pressurized NF treatment, the adoption of submerged NF treatment should be carefully considered depending on local PFAS regulations and PFAS occurrence in source water. In addition, this study did not assess the two lowest MW PFCAs, perfluorobutanoic acid ($C_4HF_7O_2$) and perfluoropentanoic acid ($C_5HF_9O_2$). Our findings reveal that the rejection of PFCAs is relatively high because of the presence of carboxylate ions. However, considering that size exclusion is also one of the most dominant mechanisms governing PFAS rejection, further comprehensive evaluations, including for perfluorobutanoic acid perfluoropentanoic acid, may be needed to ensure compliance with stringent water quality regulations.

3. Conclusions

This study investigated the factors that influence the removal of nine PFASs during submerged NF treatment of ultra-filtered dam water based on an extrapolation with the removal of 46 PPCPs. The rejection of PFASs generally increased as their molecular dimension (molecular weight or minimum projection area) increased, which narrowed the clearance in the NF membrane pores. In addition, rejection between PFCAs and PFSAs varied based on differences in the intensity of electrostatic repulsion between the PFAS functional group and membrane surface. Thus, PFASs with fully dissociated carboxylate ions can be highly rejected because of high electrostatic repulsion from the carboxylate ions of the NF membranes. The presumed mechanisms were supported by the rejection trend of the PPCPs with fully dissociated carboxylate ions, which also showed high rejection. This study established criteria for estimating PFAS rejection based on PFAS properties during low-permeate flux nanofiltration.

4. Materials and methods

4.1. Chemicals

Nine PFASs (Table 1, **Supplementary Material Table S1)** were evaluated, including five PFCAs (perfluorohexanoic acid (PFHxA), perfluoroheptanoic acid (PFHpA), PFOA, PFNA, and perfluorodecanoic acid (PFDA)); three PFSAs, (perfluorobutanesulfonic acid (PFBS), PFHxS, and PFOS); and one per- and polyfluoroalkyl ether acid (PFEA) (2,3,3,3-tetrafluoro-2-<1,1,2,2,3,3,3-heptafluoropropoxy> propanoic acid) (HFPO-DA, or GenX). A stock solution of PFASs (EPA-537PDSL-R1, Wellington Laboratories Inc., Ontario, Canada) contained linear isomers of the same components at a concentration of 2000 ng/L. In addition, a total of 46 PPCPs were evaluated (Table 1). Stock solutions containing each PPCP at 1000 mg/L were prepared in methanol. Based on their properties, they were classified into four categories: (a) uncharged (≤50 % ionized), (b) positively charged, (c) zwitterion (i.e., both positively and negatively charged), and (d) negatively charged based on their charged species. The uncharged PPCPs were further classified into hydrophilic (octanol-water coefficient Log$D$ = <4.0) and hydrophobic (Log$D$ = ≥4.0) in a solution at pH 7.5. The MPA is the area of compound projection with the minimum plane of its circular disk based on the van der Waals radius.

The partial charges of PFASs were calculated by an electrostatic potential-based scheme (CHelpG) (Breneman and Wiberg, 1990) based on density functional theory (B3LYP/6–311+G(d)//B3LYP/6–311+G(d)) using the Gaussian 16 program (Frisch et al., 2016). Partial charges determined by the CHelpG scheme were less sensitive to the basis set than traditional orbital-based methods, such as Mulliken population analysis (Mulliken, 1955). A polarizable continuum model (Tomasi et al., 2005) was used for the density functional calculation in addition to the gas phase to consider the effect of the dielectric solvent on the partial charges. Partially charged ionic functional groups (-CO_2^-, -SO_2N^--, and -SO_3^-) were not sensitive to the molecular conformation. To reduce the computational cost, the conformation of each molecular geometry was not necessarily the global minimum.

4.2. Nanofiltration module and filtration system

A commercial NF membrane, NF270 (DuPont/Filmtec; Midland, MI, USA), was used for nanofiltration. The NF270 membrane was a polypiperazine-amide thin-film composite membrane with a >97 % MgSO4 removal capacity, which has been commonly used to assess PFAS removal. Two flat-sheet NF270 membrane coupons were used to fabricate a submerged NF membrane module with an effective membrane surface area of 0.0442 m^2.

The NF treatment system **(Supplementary Materials, Figure S6)** included one submerged NF membrane module in a 5.0 L polypropylene beaker. The feed solution temperature was controlled using a temperature circulator (Thermax TM-1A, AS ONE, Osaka, Japan), and the feed solution was mixed using a magnetic stirrer to minimize concentration polarization on the membrane surface. The pipe outlet of the membrane module was connected to a peristaltic pump (MP-2000, Tokyo Rikakikai; Tokyo, Japan) and pressure gage (KDM30, Krone; Tokyo, Japan) using polypropylene pipes, and the permeate was recirculated into the 5.0 L beaker or collected in a 0.5 L polypropylene beaker. The flow rate was periodically monitored using a digital balance (EK-4100i; A&D Company, Tokyo, Japan).

The pressurized NF system used to achieve a high permeate flux of 40 L/m^2 included a 5 L stainless steel feed tank, high-pressure feed pump (20NHD15Z, Nikuni; Kawasaki, Japan), NF membrane cell with an effective membrane area of 42 cm^2 (CF042, Sterlitech; Auburn, WA, USA), digital flow meters, two pressure gauges, a needle valve, and a temperature control unit coupled with a heat exchange coil (NCB-500, Tokyo Rikakikai; Tokyo, Japan).

4.3. Experimental protocols

The feed water used in the experiments described herein was dam water collected in Nagasaki, Japan. To avoid the impact of foulants on PFAS rejection, the experimental dam water underwent pre-filtration using a polysulfone ultrafiltration module with a molecular weight cut-off of 3000 Da and an effective membrane area of 0.19 m^2 (SEP-1013, Asahi Kasei; Tokyo, Japan). The feed and permeate water quality are listed in **Supplementary Materials, Table S2**. Filtration tests for PFASs and PPCPs were conducted separately. After stabilizing the water flux of the NF membrane module, the stock solution of PFASs or PPCPs was dosed into the pre-filtered dam water at concentrations of approximately 400 ng/L or 100 μg/L for each chemical, respectively. The NF treatment was performed at a permeate flux of 5.0 L/m^2/h and a feed temperature of 22 °C over one day to achieve steady-state conditions for PFAS and PPCP rejection (Liu et al., 2021). Then, the feed and permeate samples (200 mL for PFASs and 50 mL for PPCPs) were collected.

4.4. Analysis

The analysis of the nine PFAS concentrations in the permeate and feed solutions (200 mL) was performed by pretreating the solution with solid-phase extraction (SPE) using an Oasis WAX Plus Extraction Cartridge (Waters, Milford, MA, USA). SPE cartridges were washed with ammonium acetate buffer, and the PFAS were eluted in 10 mL of methanol. Before the SPE process, surrogate stock solutions containing $^{13}C_8$-PFOA, $^{13}C_9$-PFNA, $^{13}C_5$-PFHxA, $^{13}C_4$-PFHpA, $^{13}C_6$-PFDA, $^{13}C_8$-PFOS, $^{13}C_3$-PFHxS, $^{13}C_3$-PFBS, and M3-HFPO-DA (Wellington Laboratories Inc., Ontario, Canada) were spiked into each sample at 10 μg/L. PFASs in methanol were concentrated to 5.0 mL via nitrogen evaporation. Then, the PFAS concentrations were analyzed using a Xevo TQ-S micro triple quadrupole mass spectrometer (Waters) and an ACQUITY UPLC H-Class PLUS System (Waters, Massachusetts, USA). The recovery of the surrogate standards ranged from 91 to 119 %. To measure the concentrations of the three PFASs (PFOS, PFOA, and PFHxS), the samples were directly injected into the Xevo TQ-S micro triple quadrupole mass spectrometer without SPE. The detection limit for each PFAS was 1.0 ng/L. In turn, PPCP concentrations were analyzed using an ACQUNITY ultra-performance liquid chromatograph equipped with an atmospheric pressure ionization (API) tandem mass spectrometer (Waters) (Narumiya et al., 2013).

CRediT authorship contribution statement

Takahiro Fujioka: Writing – original draft, Visualization, Validation, Supervision, Investigation, Funding acquisition, Formal analysis, Conceptualization. **Haruka Takeuchi:** Writing – review & editing, Investigation. **Hironobu Tahara:** Investigation. **Hiroto Murakami:** Writing – review & editing. **Sandrine Boivin:** Writing – review & editing, Investigation.

Declaration of competing interest

The authors declare that they have no known competing financial interests or personal relationships that could have appeared to influence the work reported in this paper.

Data availability

Data will be made available on request.

Acknowledgments

This study was supported by the Japan Science and Technology (JST) Agency Science and Technology Research Partnership for Sustainable Development (SATREPS) (JPMJSA2201).

Supplementary materials

Supplementary material associated with this article can be found, in the online version, at doi:10.1016/j.wroa.2024.100233.

References

Abbasian Chaleshtari, Z., Foudazi, R, 2022. A Review on Per- and Polyfluoroalkyl Substances (PFAS) Remediation: separation mechanisms and molecular interactions. ACS ES&T Water 2 (12), 2258–2272.

Bellona, C., Drewes, J.E., 2005. The role of membrane surface charge and solute physico-chemical properties in the rejection of organic acids by NF membranes. J. Membr. Sci. 249 (1-2), 227–234.

Bellona, C., Drewes, J.E., Xu, P., Amy, G., 2004. Factors affecting the rejection of organic solutes during NF/RO treatment - A literature review. Water Res. 38 (12), 2795–2809.

Bieber, S., Snyder, S.A., Dagnino, S., Rauch-Williams, T., Drewes, J.E., 2018. Management strategies for trace organic chemicals in water – A review of international approaches. Chemosphere 195, 410–426.

Boivin, S., Fujioka, T., 2024. Membrane fouling control and contaminant removal during direct nanofiltration of surface water. Desalination 581, 117607.

Boussu, K., Van der Bruggen, B., Volodin, A., Van Haesendonck, C., Delcour, J.A., Van der Meeren, P., Vandecasteele, C., 2006. Characterization of commercial nanofiltration membranes and comparison with self-made polyethersulfone membranes. Desalination 191 (1), 245–253.

Breneman, C.M., Wiberg, K.B., 1990. Determining atom-centered monopoles from molecular electrostatic potentials. The need for high sampling density in formamide conformational analysis. J. Comput. Chem. 11 (3), 361–373.

Frisch, M.J., Trucks, G.W., Schlegel, H.B., Scuseria, G.E., Robb, M.A., Cheeseman, J.R., Scalmani, G., Barone, V., Petersson, G.A., Nakatsuji, H., Li, X., Caricato, M., Marenich, A.V., Bloino, J., Janesko, B.G., Gomperts, R., Mennucci, B., Hratchian, H. P., Ortiz, J.V., Izmaylov, A.F., Sonnenberg, J.L., Williams, Ding, F., Lipparini, F., Egidi, F., Goings, J., Peng, B., Petrone, A., Henderson, T., Ranasinghe, D., Zakrzewski, V.G., Gao, J., Rega, N., Zheng, G., Liang, W., Hada, M., Ehara, M., Toyota, K., Fukuda, R., Hasegawa, J., Ishida, M., Nakajima, T., Honda, Y., Kitao, O., Nakai, H., Vreven, T., Throssell, K., Montgomery Jr., J.A., Peralta, J.E., Ogliaro, F., Bearpark, M.J., Heyd, J.J., Brothers, E.N., Kudin, K.N., Staroverov, V.N., Keith, T.A., Kobayashi, R., Normand, J., Raghavachari, K., Rendell, A.P., Burant, J.C., Iyengar, S. S., Tomasi, J., Cossi, M., Millam, J.M., Klene, M., Adamo, C., Cammi, R., Ochterski, J. W., Martin, R.L., Morokuma, K., Farkas, O., Foresman, J.B. and Fox, D.J. (2016) Gaussian 16 Rev. A.03, Wallingford, CT.

Fujioka, T., Kodamatani, H., Nghiem, L.D., Shintani, T., 2019. Transport of N-Nitrosamines through a reverse osmosis membrane: role of molecular size and nitrogen atoms. Environ. Sci. Technol. Letters 6 (1), 44–48.

Fujioka, T., Kodamatani, H., Yujue, W., Yu, K.D., Wanjaya, E.R., Yuan, H., Fang, M., Snyder, S.A., 2020. Assessing the passage of small pesticides through reverse osmosis membranes. J. Membr. Sci. 595, 117577.

Fujioka, T., Nghiem, L.D., Khan, S.J., McDonald, J.A., Poussade, Y., Drewes, J.E., 2012. Effects of feed solution characteristics on the rejection of *N*-nitrosamines by reverse osmosis membranes. J. Membr. Sci. 409–410, 66–74.

Fujioka, T., Ngo, M.T.T., Makabe, R., Ueyama, T., Takeuchi, H., Nga, T.T.V., Bui, X.-T., Tanaka, H., 2021. Submerged nanofiltration without pre-treatment for direct advanced drinking water treatment. Chemosphere 265, 129056.

Kimura, K., Amy, G., Drewes, J., Watanabe, Y., 2003. Adsorption of hydrophobic compounds onto NF/RO membranes: an artifact leading to overestimation of rejection. J. Membr. Sci. 221 (1-2), 89–101.

Lee, T., Speth, T.F., Nadagouda, M.N., 2022. High-pressure membrane filtration processes for separation of Per- and polyfluoroalkyl substances (PFAS). Chem. Eng. J. 431, 134023.

Li, M., Sun, F., Shang, W., Zhang, X., Dong, W., Dong, Z., Zhao, S., 2021. Removal mechanisms of perfluorinated compounds (PFCs) by nanofiltration: Roles of membrane-contaminant interactions. Chem. Eng. J. 406, 126814.

Liu, C., Zhao, X., Faria, A.F., Deliz Quiñones, K.Y., Zhang, C., He, Q., Ma, J., Shen, Y., Zhi, Y., 2022. Evaluating the efficiency of nanofiltration and reverse osmosis membrane processes for the removal of per- and polyfluoroalkyl substances from water: a critical review. Sep. Purif. Technol. 302, 122161.

Liu, C.J., Strathmann, T.J., Bellona, C., 2021. Rejection of per- and polyfluoroalkyl substances (PFASs) in aqueous film-forming foam by high-pressure membranes. Water Res. 188, 116546.

Ma, Q., Lei, Q., Liu, F., Song, Z., Khusid, B., Zhang, W., 2024. Evaluation of commercial nanofiltration and reverse osmosis membrane filtration to remove per-and polyfluoroalkyl substances (PFAS): Effects of transmembrane pressures and water matrices. Water Environ. Res. 96 (2), e10983.

Mastropietro, T.F., Bruno, R., Pardo, E., Armentano, D., 2021. Reverse osmosis and nanofiltration membranes for highly efficient PFASs removal: overview, challenges and future perspectives. Dalton. Trans. 50 (16), 5398–5410.

Mohammad, A.W., Teow, Y.H., Ang, W.L., Chung, Y.T., Oatley-Radcliffe, D.L., Hilal, N., 2015. Nanofiltration membranes review: Recent advances and future prospects. Desalination 356, 226–254.

Mulliken, R.S., 1955. Electronic population analysis on LCAO–MO molecular wave functions. I. J. Chem. Phys. 23 (10), 1833–1840.

Narumiya, M., Nakada, N., Yamashita, N., Tanaka, H., 2013. Phase distribution and removal of pharmaceuticals and personal care products during anaerobic sludge digestion. J. Hazard. Mater. 260, 305–312.
Nghiem, L.D., Schäfer, A.I., Elimelech, M., 2006. Role of electrostatic interactions in the retention of pharmaceutically active contaminants by a loose nanofiltration membrane. J. Membr. Sci. 286 (1-2), 52–59.
Pramanik, B.K., Pramanik, S.K., Sarker, D.C., Suja, F., 2017. Removal of emerging perfluorooctanoic acid and perfluorooctane sulfonate contaminants from lake water. Environ. Technol. 38 (15), 1937–1942.
Safulko, A., Cath, T.Y., Li, F., Tajdini, B., Boyd, M., Huehmer, R.P., Bellona, C., 2023. Rejection of perfluoroalkyl acids by nanofiltration and reverse osmosis in a high-recovery closed-circuit membrane filtration system. Sep. Purif. Technol. 326, 124867.
Steinle-Darling, E., Reinhard, M., 2008. Nanofiltration for trace organic contaminant removal: structure, solution, and membrane fouling effects on the rejection of perfluorochemicals. Environ. Sci. Technol. 42 (14), 5292–5297.
Tang, C.Y., Fu, Q.S., Criddle, C.S., Leckie, J.O., 2007. Effect of flux (Transmembrane Pressure) and membrane properties on fouling and rejection of reverse osmosis and nanofiltration membranes treating perfluorooctane sulfonate containing wastewater. Environ. Sci. Technol. 41 (6), 2008–2014.
Tomasi, J., Mennucci, B., Cammi, R., 2005. Quantum mechanical continuum solvation models. Chem. Rev. 105 (8), 2999–3094.
Toure, H., Anwar Sadmani, A.H.M., 2019. Nanofiltration of perfluorooctanoic acid and perfluorooctane sulfonic acid as a function of water matrix properties. Water Supply 19 (8), 2199–2205.
Tu, K.L., Chivas, A.R., Nghiem, L.D., 2011. Effects of membrane fouling and scaling on boron rejection by nanofiltration and reverse osmosis membranes. Desalination 279 (1-3), 269–277.
Verliefde, A.R.D., Cornelissen, E.R., Heijman, S.G.J., Verberk, J.Q.J.C., Amy, G.L., Van der Bruggen, B., van Dijk, J.C., 2008a. The role of electrostatic interactions on the rejection of organic solutes in aqueous solutions with nanofiltration. J. Membr. Sci. 322 (1), 52–66.
Verliefde, A.R.D., Heijman, S.G.J., Cornelissen, E.R., Amy, G.L., Van der Bruggen, B., van Dijk, J.C., 2008b. Rejection of trace organic pollutants with high pressure membranes (NF/RO). Environ. Prog. 27 (2), 180–188.
Wang, H., Zeng, J., Dai, R., Wang, Z., 2024. Understanding rejection mechanisms of trace organic contaminants by polyamide membranes via data-knowledge codriven machine learning. Environ. Sci. Technol.
Wijmans, J.G., Baker, R.W., 1995. The solution-diffusion model: a review. J. Membr. Sci. 107 (1–2), 1–21.
Zeidabadi, F.A., Esfahani, E.B., Mohseni, M., 2023. Effects of water matrix on per- and poly-fluoroalkyl substances (PFAS) treatment: Physical-separation and degradation processes – A review. J. Hazard. Mater. Adv. 10, 100322.
Zhi, Y., Zhao, X., Qian, S., Faria, A.F., Lu, X., Wang, X., Li, W., Han, L., Tao, Z., He, Q., Ma, J., Liu, C., 2022. Removing emerging perfluoroalkyl ether acids and fluorotelomer sulfonates from water by nanofiltration membranes: Insights into performance and underlying mechanisms. Sep. Purif. Technol. 298, 121648.
Zhou, C., Luo, Y., Xiong, K., Shao, S., 2023. A low-maintenance process for decentralized water purification using nanofiltration operated at ultralow flux. Sep. Purif. Technol. 327, 124869.